

1
2
3 **A Conserved Amphipathic Ligand Binding Region Influences K-Path Dependent**
4
5 **Activity of Cytochrome *c* Oxidase.**
6
7

8
9
10 †This work was supported by NIH GM26916 (SF-M).
11
12

13
14
15 Carrie Hiser¹, Leann Buhrow¹, Jian Liu, Leslie Kuhn and Shelagh Ferguson-Miller*
16

17 Department of Biochemistry and Molecular Biology, Michigan State University, East
18

19 Lansing, Michigan 48824, USA
20
21

22
23
24 *Corresponding author; phone: (517)-355-0199; email: fergus20@msu.edu
25
26

27 ¹These authors contributed equally to this work.
28
29
30
31
32
33
34
35
36
37
38
39
40
41
42
43
44
45
46
47
48
49
50
51
52
53
54
55
56
57
58
59
60

ABBREVIATIONS

BovCcO, CcO from *Bos taurus* (bovine heart); BR, bilirubin; CcO, cytochrome *c* oxidase; chenoDOC, chenodeoxycholate; CHS, cholesteryl hemisuccinate; DDM, dodecyl maltoside (lauryl maltoside); DM, decyl maltoside; DOC, deoxycholate; ET, electron transfer; glycochenoDOC, glycochenodeoxycholate; GUDCA, glyoursodeoxycholate; lyso-PC, 18:1 lyso-phosphatidylcholine (lyso-oleoyl phosphatidylcholine); PDB, Protein Data Bank; *PdCcO*, CcO from *Paracoccus denitrificans*; PPIX, protoporphyrin IX; *Rs*, *Rhodobacter sphaeroides*; *RsCcO*, CcO from *Rhodobacter sphaeroides*; TN, turnover number (electrons per second per CcO molecule); ursoDOC, ursodeoxycholate; WT, wildtype.

ABSTRACT

A conserved, crystallographically-defined bile acid binding site was originally identified in the membrane domain of mammalian and bacterial cytochrome *c* oxidase (CcO). Current studies show other amphipathic molecules including detergents, fatty acids, steroids, and porphyrins bind to this site and affect the already 50% inhibited activity of the E101A mutant of *Rhodobacter sphaeroides* CcO, as well as altering the activity of wildtype and bovine enzymes. Dodecyl maltoside, Triton X100, C12E8, lysophosphatidylcholine and CHOBIMALT detergents further inhibit *RsCcO* E101A, with lesser inhibition observed in wildtype. The detergent inhibition is overcome in the presence of μM concentrations of steroids and porphyrin analogs including deoxycholate, cholesteryl hemisuccinate, bilirubin, and protoporphyrin IX. In addition to alleviating detergent inhibition, amphipathic carboxylates including arachidonic, docosahexanoic, and phytanic acids stimulate the activity of E101A to wildtype levels by providing the missing carboxyl group. Computational modeling of dodecyl maltoside, bilirubin, and protoporphyrin IX into the conserved steroid site shows energetically favorable binding modes for these ligands and suggests that a groove at the interface of subunit I and II, including the entrance to the K-path and helix VIII of subunit I, mediates the observed competitive ligand interactions involving two overlapping sites. Spectral analysis indicates that ligand binding to this region affects CcO activity by altering the K-path dependent electron transfer equilibrium between heme *a* and heme *a*₃. The high affinity and specificity of a number of compounds for this region, and its conservation and impact on CcO activity, support its physiological significance.

1
2
3
4
5
6 The recent observations of specific conserved lipid binding sites in high-
7
8 resolution X-ray structures of cytochrome *c* oxidase¹⁻⁵ expands our vision of how lipidic
9
10 ligands may control the activity of membrane proteins⁶ and offers an explanation for
11
12 earlier reports of lipid and detergent effects on CcO activity.⁷⁻¹¹
13
14

15 An interesting finding in this regard is that cholate, a bile acid detergent that is
16
17 used to purify bovine CcO (bovCcO) and observed to strongly inhibit the enzyme¹² is
18
19 resolved in all crystal structures of the bovine enzyme (e.g.,¹; PDB: 10CC, 2DYR,
20
21 3AG2, 2Y69). One of the two best-resolved cholate binding sites is close to the entrance
22
23 of the K-path, a proton uptake pathway that is essential for activity. This cholate
24
25 molecule forms a tight hydrogen bond with the carboxyl group of E62, homologous to
26
27 E101 in the *Rhodobacter sphaeroides* CcO (*RsCcO*). This conserved residue is found by
28
29 mutagenesis to be important in K-path function.¹³⁻¹⁶ The positioning suggests that the
30
31 inhibitory effect of cholate observed in bovine CcO is due to blockage of the K-path,
32
33 preventing the proton uptake that is required to support electron transfer from heme *a* to
34
35 heme *a*₃.^{13, 17-19}
36
37
38
39
40

41 When cholate was first noted in the bovCcO structure, the idea was put forward
42
43 that it could represent an adenine nucleotide binding site.¹ Adenine nucleotides had been
44
45 observed to regulate the activity of the mammalian enzyme,²⁰⁻²⁵ although inhibition or
46
47 regulation of the K-path was not suggested at that time.
48
49

50 Removal of the carboxyl group of E101 in subunit II by mutagenesis inhibits K-
51
52 path function.¹³ Under standard assay conditions, the activity of the E101A mutant of
53
54
55
56
57
58
59
60

1
2
3 *RsCcO* is 5-8% of wildtype (WT) *CcO*.^{14, 16} Unexpectedly it was discovered that μM
4 levels of cholate or deoxycholate (DOC) stimulated the activity of this mutant by 10-fold.
5
6
7
8
9
10
11
12
13
14
15
16
17
18
19
20
21
22
23
24
25
26
27
28
29
30
31
32
33
34
35
36
37
38
39
40
41
42
43
44
45
46
47
48
49
50
51
52
53
54
55
56
57
58
59
60

^{16, 26} The apparent chemical rescue of the mutant's activity at such low concentrations suggested that these bile acids were binding close to the missing carboxyl group at the right position to serve as the needed proton acceptor/donator in the K-path. Indeed, crystals of *RsCcO* grown in the presence of DOC showed a single DOC molecule bound as expected for chemical rescue, with its carboxyl group located close to that of E101 and in a similar location as cholate in the *bovCcO*.²⁶ The conservation of a bile acid/steroid binding site in such a key position added weight to the concept that this site may have physiological significance.

To further investigate the nature and significance of this conserved site in *CcO*, we have used the *RsCcO* mutant E101A as a sensitive assay system for compounds that bind in the site, as indicated by activation, inhibition or competition. In the absence of high resolution crystal structures of *RsCcO* with other lipidic regulatory molecules besides bile acids in this site, we have characterized the site computationally and determined favorable binding modes for other observed ligands. The results show that a number of amphipathic molecules, lipids, and detergents compete in the μM concentration range, causing loss or regain of *CcO* activity via specific interactions at or near this critical conserved site at the entrance of the K-path.

MATERIALS AND METHODS

1
2
3 **Purification of CcO.** *Rhodobacter sphaeroides* strains overexpressing the 37-2
4 WT CcO²⁷ or the E101A mutant CcO¹⁶ were grown and cell membranes were prepared as
5 described²⁷ and the *RsCcO* was isolated by metal affinity chromatography as described
6 for crystallography.¹⁶ Bovine heart CcO was purified according to Suarez *et al.*²⁸
7
8
9
10
11

12 **Activity Assays.** Oxygen uptake rates were measured with a Clark-type electrode
13 and turnover rates (TN, electrons per second per CcO molecule) calculated as
14 described.²⁹ Assay mixtures contained 100 mM HEPES pH 7.4, 24 mM KCl, 2.8 mM
15 ascorbate, 5.6 μ M EDTA, 1 mM N,N,N',N'-tetramethyl-*p*-phenylenediamine (TMPD)
16 with 30 μ M bovine heart cytochrome *c* as the substrate, and with varying levels of
17 dodecyl maltoside (DDM; 0.06% final concentration was used in the "standard" assay)
18 and other additives as noted. Higher EDTA levels were tested in the assay, but did not
19 affect the behavior of WT or mutant CcO with or without added ligands.
20
21
22
23
24
25
26
27
28
29
30
31

32 The additives used in activity studies include: lyso-oleoyl phosphatidylcholine
33 (18:1 lysophosphatidylcholine, lyso-PC) and asolectin from Avanti Polar Lipids
34 (Alabaster, AL), high-purity 10% Triton X100 from ThermoScientific/Pierce (Rockford,
35 IL), arachidonic and docosahexanoic acids from Cayman Chemicals (Ann Arbor, MI),
36 and CHOBIMALT, DDM, decyl maltoside (DM), and Anapoe 20 (Tween 20) from
37 Anatrace/Affymetrix (Maumee, OH). Other additives were from Sigma-Aldrich
38 (St.Louis, MO). The chemicals structures of all additives are listed in Supporting Table
39 T1.
40
41
42
43
44
45
46
47
48
49
50

51 **Spectral Reduction Assays.** The steady-state reduction levels of hemes were
52 compared by using a variation of the method of Konstantinov *et al.*¹⁷ Assays were
53
54
55
56
57
58
59
60

1
2
3 performed in 100mM CHES pH 9.5, with 0.01% DDM, 1 mM ascorbate and 200 μ M
4
5
6
7
8
9
10
11
12
13
14
15
16
17
18
19
20
21
22
23
24
25
26
27
28
29
30
31
32
33
34
35
36
37
38
39
40
41
42
43
44
45
46
47
48
49
50
51
52
53
54
55
56
57
58
59
60

performed in 100mM CHES pH 9.5, with 0.01% DDM, 1 mM ascorbate and 200 μ M
TMPD, with and without CHOBIMALT, in an unstirred cuvette in a Perkin-Elmer
Lambda 40 spectrophotometer. Curves were aligned to 462 nm and 621 nm for the Soret
and α peaks, respectively, then normalized to the fully reduced α peak (607 nm-minus-
630 nm, indicative of enzyme concentration) so that different enzymes and conditions
could be compared.¹⁷

Protein and Ligand Structures. The crystal structures of bovine CcO (PDB:
2DYR⁵), *RsCcO* with (PDB: 3DTU²⁶) and without (PDB: 2GSM²) deoxycholate, and
Paracoccus denitrificans CcO (PDB: 3HB3⁴) were used for ligand binding and flexibility
analysis. Crystal structures of ferrochelatase in complex with cholate (PDB: 2PO7³⁰) or
heme (PDB: 2QD2³¹) and serum albumin in complex with biliverdin (PDB: 2VUE³²) or
fusidic acid (PDB: 2VUF³²) were used for ligand docking. Decyl maltoside, dodecyl
maltoside, biliverdin, and protoporphyrin IX ligand structures were obtained from the
above structures.

SLIDE Small Molecule Docking. The groove between subunits I and II in the
crystal structure of *RsCcO* with bound deoxycholate removed (PDB: 3DTU²⁶) was used
as the target for *SLIDE* (Screening Ligands by Induced-fit Docking, Efficiency)
prediction of the binding modes of experimentally identified ligands.^{33, 34} *SLIDE*
characterizes a binding pocket by a template of chemistry-labeled points that are
favorable positions for protein-ligand hydrophobic interactions or hydrogen bonds. In
this work, the known interactions of deoxycholate or dodecyl maltoside were used to
create the template. To sample ligand flexibility fully, low energy conformations of all

1
2
3 docked ligands were generated using *Omega* (OMEGA version 2.0. OpenEye Scientific
4 Software, Santa Fe, NM³⁵). Using distance and geometric constraints, *SLIDE* predicts the
5 orientation of ligand binding by sampling all orientations that yield good shape and
6 chemical complementarity between the ligand and protein, then chooses the orientation of
7 the conformer with the most favorable $\Delta G_{\text{binding}}$ according to *SLIDE*'s OrientScore
8 (Tonero *et al.*, *in preparation*). *SLIDE* AffiScore, a weighted sum of favorable polar and
9 hydrophobic interactions and unfavorable (unsatisfied/repulsive) interactions between the
10 protein and ligand, was used to assess the relative $\Delta G_{\text{binding}}$ of these diverse ligands in the
11 binding groove.
12
13
14
15
16
17
18
19
20
21
22
23

24 **Ligand Transposition.** To test whether porphyrin-like ligands could mimic the
25 steroid ring interaction in *RsCcO*, comparisons were made to other proteins in which both
26 these types of ligands have been found to occupy the same site. Serum albumin and
27 ferrochelatase have been crystallized in separate complexes with steroid and heme-like
28 ligands in a single binding site (see Protein and Ligand Structures, above). The overlaid
29 ligands were transposed into the *RsCcO* steroid site, in the same orientation as they
30 exhibit in serum albumin and ferrochelatase. The bound cholate in ferrochelatase (PDB:
31 2PO7³⁰) and bound fusidic acid in serum albumin (PDB: 2VUF³²) were aligned to the
32 *RsCcO* deoxycholate (PDB: 3DTU²⁶) based on least-squares fitting of their steroid ring
33 atoms using *OEChem RMSD* (RMSD version 1.7.2.4. OpenEye Scientific Software,
34 Santa Fe, NM³⁵). Ferrochelatase with bound protoporphyrin IX (PDB: 2QD2³¹) was
35 superimposed onto ferrochelatase with bound cholate, and serum albumin with bound
36 biliverdin (PDB: 2VUE³²) was superimposed onto serum albumin with bound fusidic
37
38
39
40
41
42
43
44
45
46
47
48
49
50
51
52
53
54
55
56
57
58
59
60

1
2
3 acid (PDB:2VUF³²), based on least-squares fitting of their protein backbone atoms using
4
5 *PyMOL* molecular graphics software (Schrödinger, Inc., New York, NY). Whether the
6
7 heme ligands were sterically permitted and energetically favorable in this orientation was
8
9 then assessed using *PyMOL* and *SLIDE* prediction of $\Delta G_{\text{binding}}$, respectively.
10
11

12 ***Consurf* Amino Acid Conservation and *ProFlex* Flexibility Analysis.** The
13
14 amino acid conservation and flexibility of the CcO main chain was evaluated using the
15
16 *Consurf*³⁶ and *ProFlex*³⁷ methods, respectively, as described in Buhrow *et al.*³⁸ Over
17
18 250 amino acid sequences of CcO were used for conservation analyses as described in
19
20 Buhrow *et al.*³⁸
21
22
23
24
25
26

27 RESULTS

28
29 **Bile Acid Structural Specificity for Stimulating E101A *RsCcO* Activity.** To
30
31 elucidate the structural specificity for the observed stimulation of the E101A mutant of
32
33 *RsCcO*, activity was measured with a variety of bile acids at 250 μM final concentration
34
35 under standard assay conditions (Table 1). The effect on E101A activity was highly
36
37 sensitive to the position and stereochemistry of hydroxyl groups on the steroid ring and to
38
39 the length of the carboxyl tail (Supporting Table T1). Cholate and deoxycholate²⁶
40
41 remained the strongest effectors at this concentration. Only chenoDOC and lithocholate
42
43 were close to their effectiveness (~10 fold stimulation); taurocholate stimulated only 3-
44
45 fold and GUDCA stimulated by 40%. UrsoDOC and glycochenoDOC had no observable
46
47 effect. The most potent effector, deoxycholate (Figure 1), caused no change in the
48
49 spectral properties of oxidized or reduced E101A. All the bile acids tested had no
50
51
52
53
54
55
56
57
58
59
60

1
2
3 significant effect on WT *RsCcO* activity at 250 μM concentration under these conditions.
4
5
6 Their differential effect on the mutant presumably was due to their ability to chemically
7
8 rescue the missing carboxyl group in E101A, involved in proton uptake at the entrance of
9
10 the K-path where crystal structures show bile acids to bind.
11

12 **Other Lipidic and Heterocyclic Compounds Affect E101A *RsCcO* Activity.**

13
14
15 Other lipidic and heterocyclic compounds with carboxyl functional groups were tested
16
17 for their ability to differentially stimulate the activity of E101A under the standard assay
18
19 conditions (Figure 1A). Among those tested, the cholesterol mimic cholesteryl
20
21 hemisuccinate (CHS) stimulated E101A even more effectively than cholate, to an activity
22
23 of $\sim 500 \text{ s}^{-1}$ with half-maximal stimulation ($K_{1/2}$) at $\sim 80 \mu\text{M}$, as compared to 200 μM for
24
25 cholate. Since some structural and binding similarities between porphyrins and steroids
26
27 have been observed (ferrochelatase, serum albumin, heme oxygenase³⁰⁻³²), the heme
28
29 precursor protoporphyrin IX (PPIX) was tested. It also stimulated E101A more potently
30
31 than bile acids ($K_{1/2} \sim 14 \mu\text{M}$); the heme breakdown product bilirubin (BR) stimulated to a
32
33 lesser degree (to $\sim 180 \text{ s}^{-1}$ with $K_{1/2} \sim 50 \mu\text{M}$).
34
35
36
37
38

39 Bile acids, PPIX, BR, and CHS had no significant effect on the activity of the
40
41 D132A mutant of *RsCcO* (data not shown), even though mutation of that carboxyl group
42
43 at the entrance of the D proton uptake pathway had been previously shown to be very
44
45 effectively rescued by arachidonic and docosahexanoic acids but not the corresponding
46
47 alcohols.³⁹ Although the steroid/porphyrin-related compounds did not rescue D132A, the
48
49 long chain unsaturated fatty acids were tested and found to rescue E101A as well as
50
51 D132A (Figure 1B). Therefore the steroid binding appears quite specific for the K-path
52
53
54
55
56
57
58
59
60

1
2
3 entrance region, while the more flexible long-chain fatty acids show high affinity for the
4
5 vicinity of both proton entry pathways.
6
7

8 As in the case of the long-chain fatty-acids arachidonic and docosahexanoic acids
9
10 (Figure 1B), the 20-carbon branched-chain isoprene compound phytanic acid, known to
11 modulate pathways of steroid and lipid synthesis,⁴⁰⁻⁴² was found to be a surprisingly
12 powerful effector of E101A (Figure 1B), stimulating to an activity of $>1000 \text{ s}^{-1}$ ($\sim 20\times$
13 non-additive rates) with half-maximal stimulation at $\sim 4 \mu\text{M}$. Phytol, a phytanic acid
14 precursor without a carboxyl group, had little effect at the same μM concentrations and,
15 as seen with the bile acids, phytanic acid at μM levels did not stimulate the D132A
16 mutant (data not shown). Retinoic acid, another isoprene compound and known regulator
17 of lipid and steroid metabolism,⁴³ also strongly stimulated E101A activity ($K_{1/2} \sim 8 \mu\text{M}$)
18 (Figure 1B) with little effect on D132A or WT activity (data not shown). The high
19 affinity ligands shown in panel B stimulated to close to WT activity, indicating strong
20 repair of the carboxyl mutation.
21
22
23
24
25
26
27
28
29
30
31
32
33
34
35

36 These results (Figure 1A,B), including the differential selectivity of the D- and K-
37 path chemical rescue, indicate a significant difference in the binding site characteristics
38 of the two proton pathway entrance regions. The D-path associated binding site (whose
39 exact location is not known) appears more constricted, only accommodating unbranched
40 functional groups, while the K-path binding site appears substantially larger,
41 accommodating not only long-chain polyunsaturated fatty acids but also steroids,
42
43
44
45
46
47
48
49
50
51
52
53
54
55
56
57
58
59
60

The Detergent Dodecyl β -D-Maltopyranoside (DDM) Strongly Inhibits

E101A Activity. During these studies it was discovered that not only the amphiphilic carboxylate molecules discussed above were capable of modifying the E101A mutant's activity, but also the detergent DDM itself. DDM is routinely used to solubilize and assay CcO since the original finding that it was uniquely effective in dispersing, stabilizing and activating CcO.⁴⁴ However, DDM inhibited the E101A mutant even at the relatively low levels (0.06%) normally used for maximally activating the WT *RsCcO* (Figure 2A). Decyl β -D-maltopyranoside (DM) with the same maltose headgroup but shorter alkyl chain was less inhibitory than DDM, but the α and β isomers of DDM had similar effects (data not shown). This indicates that the chain length of the detergent was influential in the effect on E101A activity.

The inhibitory effect of DDM on E101A activity, in contrast to little effect on WT (Figure 2A) or D132A (data not shown), suggests that DDM can bind in the vicinity of the bile acid/steroid site in the E101A mutant and interfere further with the mutant's already inhibited activity (~50% of WT). Therefore DDM appears to compete with other amphipathic ligands, thus complicating the interpretation of the mutant-based assay. The mutant's activity in the presence of any added ligand is then expected to reflect both the ligand's ability to compete with DDM for binding (hence removal of detergent inhibition) and the ligand's own effect once bound (activation or inhibition or both).

Effects of Carboxylate Ligands on E101A Are Altered in Low DDM. To

determine the nature of the effect of DDM concentration, ligands were re-tested in 0.01% DDM, the minimal level required to support enzyme solubility and activity (Figure 2B).

1
2
3 Under these low DDM conditions without any additives, the E101A mutant was much
4 more active, showing ~50% of WT activity in 0.01% DDM compared to 5-8% of WT
5
6 activity in 0.06% DDM (Figure 2A). Indeed, some of the additives that had stimulated
7
8 the activity of the mutant in 0.06% DDM now inhibited when tested at low DDM (Figure
9
10 2B). However, in several cases (e.g., cholesterol hemisuccinate, retinoic acid)
11
12 stimulation still occurred at low ligand concentrations before inhibition set in, suggesting
13
14 a complex mode of interaction (see Discussion). It is worth noting that a biphasic ligand
15
16 effect of stimulation followed by inhibition in the mM concentration range was also
17
18 observed for some ligands even in the higher DDM conditions. Ligand interactions with
19
20 WT *RsCcO* were less affected by DDM concentration (data not shown).
21
22
23
24
25

26
27 The soybean phospholipid mixture (asolectin) also stimulated and then inhibited
28
29 in the 200 – 1000 μM range, but likely components of this mixture, including cardiolipin
30
31 and dioleoyl phosphatidylcholine, when tested individually were inhibitory rather than
32
33 stimulatory (data not shown). The results suggest that the presence of low levels of much
34
35 more potent effectors, such as long chain fatty acids, account for the asolectin effects.
36
37
38

39 **Other Detergents Inhibit E101A Activity and Wildtype to a Lesser Extent.**

40
41 The generality of the differential inhibitory effects of DDM on E101A versus WT *CcO*
42
43 was investigated. The detergent Triton X100 was previously established as an inhibitor
44
45 of *bovCcO*.^{19, 45} This detergent strongly inhibited E101A activity ($K_{1/2}$ ~50 μM) when
46
47 assayed at the lowest level of DDM (0.01%) (Figure 3A). Unlike DDM, Triton X100
48
49 also inhibited the activity of WT *RsCcO* ($K_{1/2}$ ~200 μM) but to a lesser extent (Figure
50
51 3B). Inhibition of E101A occurred well below the critical micelle concentration of
52
53
54
55
56
57
58
59
60

1
2
3 Triton X100 (230 μM), suggesting that the effect was mediated by Triton X100
4
5 monomers rather than by Triton X100 micelles. Neither Triton X100 nor DDM inhibited
6
7 the D-path mutant D132A (data not shown), supporting the selective interaction of Triton
8
9 X100 and DDM at the K-path, which is not rate-limiting in the D-path mutant.
10
11

12
13 The three cholesterol-based detergents digitonin, CHAPS, and CHOBIMALT
14
15 might be expected to have some affinity for the steroid site. However, CHAPS had been
16
17 shown to have no effect.¹⁶ CHOBIMALT is potentially a better analog of cholesterol
18
19 since its bi-maltose headgroup is attached to the single hydroxyl on the A-ring of
20
21 cholesterol.⁴⁶ The activity of E101A was strongly inhibited by CHOBIMALT, even
22
23 more potently than by DDM or Triton X100, with half-maximal inhibition at ~ 2 μM in
24
25 0.01% DDM (Figure 3A). WT *R_sCcO* activity was also inhibited, but 100-fold less with
26
27 half-maximal inhibition at ~ 200 μM in 0.01% DDM (Figure 3B). Digitonin, with its very
28
29 large branched sugar head group and modified steroid ring structure, was a less powerful
30
31 inhibitor, with $K_{1/2}$ in the 200 μM range (data not shown).
32
33
34
35

36
37 Lyso-oleoyl phosphatidycholine (lyso-PC) has detergent characteristics and was
38
39 reported to stimulate *bovCcO*.^{10, 11} However, lyso-PC inhibited E101A in 0.01% DDM
40
41 with half-maximal inhibition at ~ 17 μM (Figure 3A). It had little effect on WT *R_sCcO* in
42
43 high (data not shown) or low DDM (Figure 3B) and no significant effect on E101A in
44
45 0.06% DDM (Figure 3C). Since lyso-PC strongly inhibited E101A only at the lower
46
47 DDM concentrations, it appeared to compete at the K-path site. Similarly strong
48
49 inhibition of E101A was observed for the detergent C12E8 in low DDM (Figure 3A),
50
51 with little effect on WT (Figure 3B) or at high DDM (Figure 3C). The effects of all these
52
53
54
55
56
57
58
59
60

1
2
3 inhibitory detergents at high DDM appears insignificant (Figure 3C) due to the already
4
5 low activity of the mutant E101A in 0.06% DDM. However, their effects provide a
6
7 dramatic contrast to Tween 20, which was a remarkable exception to the general rule of
8
9 strong inhibitory effects on E101A of non-carboxylate detergents. Tween 20 has a 12
10
11 carbon alkyl tail like DDM or C12E8, but a bulky branched polyoxyethylene head group,
12
13 unlike the long linear polyoxyethylene ether chains of Triton X100 and C12E8. Instead
14
15 of inhibiting, it dramatically stimulated the activity of E101A at all DDM concentrations
16
17 (Figure 3A,C). A model to explain this behavior in terms of adjacent and somewhat
18
19 overlapping binding sites is discussed below.
20
21
22
23

24 **Non-Carboxylate Detergents Compete with Deoxycholate for Binding.** The
25
26 differential effects on E101A compared to WT *RsCcO* of all the amphipathic ligands
27
28 tested, with and without carboxylate groups, suggest that their binding behavior is
29
30 strongly influenced by the change in chemistry at the mouth of the K-path with the loss of
31
32 the E101 carboxyl group. This leads to the conclusion that they are exerting their effects
33
34 by binding in the vicinity of the steroid/bile acid site. So far the position of that site has
35
36 only been defined crystallographically for DOC in the WT *RsCcO*.²⁶ While
37
38 crystallization with the other amphipathic effectors of *RsCcO* and the E101A mutant is
39
40 currently in progress, some of these ligands were tested for competitive binding at the
41
42 same site as DOC by comparing their effects on the activity of E101A in the absence or
43
44 presence of 300 μ M DOC. This DOC concentration had a minor activating effect on
45
46 E101A in 0.01% DDM (Figure 2B) for which a correction was made. The detergents
47
48 Triton X100 and CHOBIMALT were chosen for competition studies because of their
49
50
51
52
53
54
55
56
57
58
59
60

1
2
3 strong inhibitory effects (Figure 3). Triton X100 clearly inhibited E101A less effectively
4
5 in the presence of DOC ($K_{1/2} \sim 200 \mu\text{M}$) than in its absence ($K_{1/2} \sim 50 \mu\text{M}$) (Figure 4A).
6
7 Similarly, in the presence of $100 \mu\text{M}$ Triton X100, DOC was less effective at stimulating
8
9 E101A (data not shown). CHOBIMALT also inhibited E101A much less effectively in
10
11 the presence of DOC ($K_{1/2} \sim 50 \mu\text{M}$) than in its absence ($K_{1/2} \sim 5 \mu\text{M}$) (Figure 4B),
12
13 indicating that both Triton X100 and CHOBIMALT compete with DOC for binding to
14
15 the steroid site.
16
17
18
19

20 Mechanism of Inhibition/Activation of CcO by Amphipathic K-Path

21
22 **Ligands.** A number of earlier studies have established that the electron transfer
23
24 equilibrium between heme *a* and heme *a*₃ in bovcCo is inhibited by detergents, including
25
26 Triton X100¹⁹, DDM,¹⁹ and cholate.¹² The inhibition has been attributed to blockage of
27
28 the K-path, which is required for proton uptake to stabilize the reduced state of heme *a*₃.
29
30 A similar type of inhibition is observed in the case of K-path mutations.^{13, 14, 17, 18} To
31
32 determine whether alteration of this equilibrium could explain the inhibitory and
33
34 stimulatory effects of the ligands studied here, a steady-state spectrophotometric
35
36 method¹⁷ was used to assay the relative levels of reduction of the heme groups in the
37
38 presence and absence of ligand. The steady-state levels of heme *a* and heme *a*₃ reduction
39
40 were measured by comparing the relative absorbances of the α peak at 607 nm
41
42 (absorbance contributed approximately 80% by heme *a*⁴⁷) and the Soret peak at 445 nm
43
44 (absorbance due to approximately 50% heme *a* and 50% heme *a*₃⁴⁷) (Figure 5). For the
45
46 WT *R*sCcO, the change in absorbance of the α and Soret peaks was similar (indicating
47
48 29% and 26% reduction, respectively, of the associated hemes), suggesting that the
49
50
51
52
53
54
55
56
57
58
59
60

1
2
3 steady-state equilibrium favored some electron retention on heme *a* at the high pH
4
5 necessary to slow the activity of the WT to observe a steady-state. For the E101A under
6
7 the same conditions, the α peak was more affected (indicating ~51% reduction of
8
9 associated hemes) than the Soret peak (indicating ~26% reduction), supporting the
10
11 hypothesis that this mutation alone favored electron retention on heme *a*. Addition of
12
13 CHOBIMALT to WT also had a selective effect on the α peak (~43% reduction of
14
15 associated hemes) implying that the binding of this detergent also impaired ET from
16
17 heme *a* to *a*₃. Addition of CHOBIMALT to E101A influenced the equilibrium even
18
19 further, leading to a strong effect on the α peak (indicating ~73% reduction of associated
20
21 hemes) while the Soret peak was affected only to an extent that was accountable by
22
23 preferential heme *a* reduction (~44%) in the steady state. It should be noted that in the
24
25 fully reduced and fully oxidized states, the addition of CHOBIMALT did not affect the
26
27 spectra of either WT or E101A. The results are consistent with an inhibitory effect of
28
29 these E101A ligands on the electron transport equilibrium between the hemes,
30
31 presumably due to effects on the proton uptake required for heme *a*₃ – Cu_B reduction.
32
33
34
35
36
37

38
39 **Modeling Alternative Ligand Interactions at the Steroid Site Based on Other**
40
41 **Crystal Structures.** Given the variety of compounds that appear to interact with
42
43 relatively high affinity at what was originally observed to be a bile acid/steroid binding
44
45 site, it is important to note that other structurally characterized proteins show
46
47 interchangeability of ligands, in particular steroids, porphyrins and other amphipathic
48
49 molecules.³⁰⁻³² Knowledge of how porphyrin and steroid molecules bind relative to one
50
51 another in the same site in another protein – mimicking each others' key protein
52
53
54
55
56
57
58
59
60

1
2
3 interactions – provides testable information regarding how they might bind relative to one
4 another in the *RsCcO* deoxycholate site. Ferrochelatase has been crystallized with its
5 substrate PPIX and the bile acid cholate,^{30, 31} showing how a steroid and porphyrin could
6 bind to the same site (Figure 6A). Similarly, human serum albumin has been crystallized
7 with biliverdin, a natively transported heme catabolic product, and fusidic acid, an
8 antibiotic that is structurally similar to bile acids, in the same binding site.³² To test
9 whether these heme-like ligands could mimic the cholate steroid ring interactions in
10 *RsCcO* in the same orientation they exhibit in serum albumin and ferrochelatase, their
11 PPIX and biliverdin ligands were transposed into the *RsCcO* bile acid/steroid binding site
12 as described in the Materials and Methods. The transposed ferrochelatase heme group
13 interpenetrated the *RsCcO* protein surface, and thus would be sterically disallowed in this
14 binding orientation, while the serum albumin biliverdin was transposed into the *RsCcO*
15 site with no steric hindrance and interacted favorably with *RsCcO* according to *SLIDE*
16 evaluation of $\Delta G_{\text{binding}}$ (Figure 6B).

17
18
19
20
21
22
23
24
25
26
27
28
29
30
31
32
33
34
35
36
37 **Docking of PPIX and BR into the Steroid Binding Site.** Alternative binding
38 interactions for these ligands in the steroid site were identified by *SLIDE* small molecule
39 docking of low energy PPIX and BR conformers. The top four PPIX dockings (scoring
40 two standard deviations greater than the average docked PPIX score) depicted two
41 possible binding modes in which half the PPIX is located in the steroid site and one
42 propionate group makes protein interactions similar to the DOC carboxyl tail (one mode
43 is shown in Figure 6C). The top eight docked BR conformers (based on *SLIDE* scores at
44 least two standard deviations above the mean) shared a single BR binding mode (Figure
45
46
47
48
49
50
51
52
53
54
55
56
57
58
59
60

1
2
3 6D). This binding mode, like that of BR in human serum albumin, creates an L-shaped
4
5 ligand conformation³² with the BR dipyrinone group located in the same site as the
6
7 steroid ring. The *SLIDE* docking of PPIX and BR support the likely interaction of these
8
9 ligands with the steroid binding site and provide testable hypotheses for ligand-protein
10
11 side chain interactions.
12
13

14 **Modeling Detergent Binding to the *RsCcO* Steroid Binding Region.**

15
16 Predicting possible binding orientations of detergents in the steroid site is currently a
17
18 significant challenge; however, an alternative interaction mode is suggested by a *PdCcO*
19
20 crystal structure containing a DDM bound in a unique orientation just above the steroid
21
22 binding site.⁴ In this structure, the maltose head group is indicated to be flexible and
23
24 located in the middle of the membrane region, while the tail is embedded in a
25
26 hydrophobic groove that is also occupied by an alkyl tail in all oxidase structures (Figure
27
28 6E). To test whether the head group of this unusual binding orientation of DDM could
29
30 also interact with the steroid site, low energy conformations of DM and DDM were
31
32 docked into the *PdCcO* DDM site by using *SLIDE*. Among the many energetically
33
34 favorable dockings identified with acyl tails occupying the *PdCcO* DDM site, the maltose
35
36 head group positions varied between being solvent-exposed or protein-associated. In the
37
38 latter cases, the *RsCcO* steroid binding site was occluded by the head group (Figure 6E).
39
40 This could explain how DDM and certain other detergents compete with bile acid binding
41
42 while occupying an equally conserved, overlapping region in close proximity. It may
43
44 also explain the inhibitory effects of the detergents on the E101A mutant, since the
45
46
47
48
49
50
51
52
53
54
55
56
57
58
59
60

1
2
3 detergent head group binding in the cholate site could interfere directly with K-path
4
5
6 proton uptake.
7

8 DISCUSSION

9
10 This work addresses the effects of various amphipathic and steroid-like molecules
11 that competitively interact at a crystallographically-defined bile acid/steroid binding site
12 located at the entrance of the K proton uptake path of bacterial and mammalian CcO. It
13 is interesting that none of the more than 50 CcO crystal structures in the PDB has any
14 ligand resolved in this site, except the additives cholate or deoxycholate. This suggests
15 that in the native structure this site is not a phospholipid binding site, since detergents
16 such as DM, DDM, or LDAO typically occupy phospholipid sites in the bacterial CcO,
17 sites which contain native lipids in the bovCcO.³
18
19
20
21
22
23
24
25
26
27
28

29 Comparing the cholate binding site in bovCcO with the DOC site in RsCcO
30 indicates that they have important structural similarities beyond their location at the
31 entrance region of the K-path (Supporting Table T2). The consensus between cholate and
32 DOC binding includes interactions with the conserved K-path residue E62/E101 (bov/Rs)
33 in subunit II, a conserved threonine T66/T105 one helical turn above this entrance point
34 of the K-path, and positive charges interacting with the carboxyl group consisting of a
35 cadmium ion or a histidine side chain (RsCcO) or a pair of arginine residues (bovCcO)
36
37
38
39
40
41
42
43
44
45
46 There is also a lipid or detergent molecule closely associated with the external
47
48 hydrophobic surface of the bile acid in each case.
49

50 Cholate in bovCcO contacts subunit VIa of the other monomer in the
51
52 crystallographic dimer, as well as the highly conserved subunit II residue W65, while
53
54
55
56
57
58
59
60

1
2
3 DOC in *RsCcO* contacts subunit I via conserved residues A319 and P358. In both cases
4
5 several water molecules are stabilized by the presence of these ligands, participating in
6
7 their interactions with subunits I and II (Figure 7).
8
9

10 **Mechanisms of Activation/Inhibition of CcO by Ligands.** There are several
11
12 potential mechanisms by which amphipathic compounds could activate or inhibit CcO by
13
14 favoring or disfavoring proton uptake in the K-path.
15
16

17
18 One hypothesis involves the disruption or stabilization by ligand binding of a
19
20 proton conducting network in the K-path, which involves hydrogen bonded amino acids
21
22 and water molecules that are likely required for proton transfer. Waters in the lower K-
23
24 path have been crystallographically resolved in *PdCcO*,⁴ *RsCcO*,^{48, 49} and *bovCcO* (PDB:
25
26 2DYZ) and a role for E101 in organizing water near the K-path entrance has been
27
28 invoked for bacterial CcOs.^{4, 6, 50} DOC binding results in three well-resolved water
29
30 molecules binding between the planar ring system of DOC and the lower K-path (Figure
31
32 7). The resulting changes in hydrogen bonding at this opening to the K-path may affect
33
34 the continuity of the pathway or reduce mobility of water molecules involved in
35
36 conducting protons.
37
38
39

40
41 Another possibility (which may coexist with the first) is that the presence of
42
43 amphipathic ligands in the region associated with the K-path may either promote or
44
45 restrict conformational change observed to occur in the reduced state,^{48, 49} which is
46
47 postulated to be necessary to open the K-path for rapid proton access to the heme a_3
48
49 region.^{38, 48, 51} The central region of the K-path (subunit I, helix VIII, residues 355-364)
50
51 has been shown by H/D exchange to experience altered solvent accessibility upon
52
53
54
55
56
57
58
59
60

1
2
3 enzyme reduction.⁵² Intrinsic protein flexibility analysis also suggests this region is
4
5 highly flexible, influencing water molecule positions along the K-path.³⁸
6
7

8 Deoxycholate appears to lower the flexibility of CcO, based upon lower average
9
10 B-values of WT *RsCcO* crystals with DOC bound.²⁶ *ProFlex* modeling also suggests that
11
12 DOC reduces conformational flexibility of the K-path region (Figure 8 C, D) relative to
13
14 the unbound state (Figure 8 A, B). In addition, upon reduction of *RsCcO* crystals there is
15
16 loss of bound DOC,⁶ suggesting that ligands like DOC may stabilize the oxidized state
17
18 and prevent conformational changes required for efficient functioning of the K-path.
19
20

21
22 **Separate but Overlapping Binding Sites for Steroids and Detergents in the**
23
24 **K-Path Region.** It is a curious observation that the site where cholate (in *bovCcO*) and
25
26 DOC (in *RsCcO*) is bound is not occupied by any other detergent or lipid molecule in all
27
28 CcO structures so far determined. Nevertheless our data strongly suggests competition
29
30 between the bile acids and certain detergents (including DDM) as well as other effector
31
32 molecules. A possible explanation for this seeming disconnect comes from the recent
33
34 *Paracoccus CcO* structure⁴ where a DDM molecule is seen with its maltose head group
35
36 sampling several positions in the membrane region (Figure 2E). Computational analysis
37
38 (Figure 6E) supports an energetically favorable position with the head group overlapping
39
40 the steroid binding site, which could explain the observed competition with molecules
41
42 binding in the steroid site. Interestingly, in *RsCcO* and *bovCcO* crystal structures, an
43
44 alkyl tail is always resolved in the deep groove where the tail of the unusual *Paracoccus*
45
46 DDM position is located (Figure 9). This region mediates the interaction between subunit
47
48 I and the highly conserved second transmembrane helix of subunit II. In *bovCcO*, the
49
50
51
52
53
54
55
56
57
58
59
60

1
2
3 alkyl tail position is occupied by the fatty acid chain of a cardiolipin molecule that
4 connects two monomers at the interface of the dimer.⁵
5
6

7
8 The working hypothesis arising from these observations is that some of the
9 effectors, particularly long chain nonionic detergents, may exert their influence by
10 binding at the upper DDM site with their head groups interacting with the lower bile
11 acid/steroid site (Figure 9) blocking the K path and competing with other ligands. The
12 strength and nature of their competing effects would depend on their head group size,
13 chemistry, positioning and occupancy in the steroid site. The exceptional activating
14 behavior of Tween 20, which has an unusually bulky branch-chain head group, can be
15 explained as due to its ability to bind to the upper alkyl chain groove but inability of its
16 head group to bind in the membrane region.
17
18
19
20
21
22
23
24
25
26
27
28

29 The presence of overlapping binding sites raises the question of which molecules
30 fit into which sites. It is predicted from docking and the available data that the bulkier
31 ligands (steroids, porphyrins, branched-chain isoprenes) bind in the lower site and the
32 longer simpler chains (DDM, the Triton X100 polyoxyethylene group, C12E8) bind in
33 the narrower groove provided by the upper site, while some (e.g., long-chain fatty acids,
34 Triton X100) occupy both. However, deciphering the actual binding specificity will
35 require further mutational and crystallographic analysis. An interesting, possibly
36 analogous site has been defined for Complex I^{53, 54} in which a critical subunit interface
37 region appears to be where quinones, inhibitors, and detergents, including Triton X100
38 and C12E8 (but not bile acids), bind at overlapping amphipathic sites.
39
40
41
42
43
44
45
46
47
48
49
50
51
52
53
54
55
56
57
58
59
60

1
2
3 **Potential Physiological Implications of the Steroid Site of CcO.** The
4
5 physiological significance of this site remains elusive, although the fact that the bile
6
7 acid/steroid site is conserved from bacteria to mammals and interacts with high affinity
8
9 with a set of physiologically interesting compounds strengthens the idea that the site is
10
11 important in regulation of cytochrome *c* oxidase activity.
12
13

14
15 Studies of purified bovine CcO support bile acids¹² as activity regulators.
16
17 Analyses of mitochondrial function have also implicated glucocorticoids⁵⁵ and steroids as
18
19 strong effectors.^{56, 57} Whole cell and tissue studies suggest that porphyrins, BR and bile
20
21 acids modulate cell fate, specifically at the level of CcO activity.^{58, 59} Together these
22
23 results suggest that the CcO steroid site is sensitive to a variety of physiological ligands
24
25 with previously uncharacterized molecular effects.
26
27

28
29 Similarly, isoprene-derived compounds such as thyroid hormone^{60, 61} have been
30
31 reported to influence CcO activity in mitochondria, findings in accord with the direct
32
33 effects of cholesteryl hemisuccinate, retinoic acid (Figures 1, 2) and thyroid hormone
34
35 (data not shown) on the purified enzyme in our studies. The observation that another
36
37 isoprene compound, phytanic acid, inhibits CcO in rat cerebral cortex homogenates at
38
39 μM levels⁶² is consistent with our finding of powerful inhibition of bacterial and
40
41 mammalian CcO.
42
43

44
45 The original suggestion, based on crystallographic¹ and activity^{20, 21, 63} studies on
46
47 the mammalian oxidase, was that the cholate sites in bovCcO represented adenine
48
49 nucleotide regulatory sites, due to the similar size, shape, and binding characteristics of
50
51
52
53
54
55
56
57
58
59
60

1
2
3 these ligands.¹ Our current studies do not rule this out, but we did not observe significant
4 effects of adenine nucleotides in the assay systems described here.
5
6

7
8 Another interesting feature of the ligand binding region we have described in this
9 work is its location at the interface of the crystallographically-defined *bovCcO* dimer.
10 The *bovCcO* structure shows a homodimer with two cholate molecules and two
11 cardiolipin molecules resolved at that interface.⁵ In fact, one alkyl chain of each
12 cardiolipin molecule is embedded in the groove we have defined as the upper site (Figure
13 9), the same site observed to bind DDM in *PdCcO*, allowing its head group to overlap the
14 steroid site. It is plausible that physiological ligands to this region could control
15 monomer/dimer equilibrium and, in turn, influence formation of the respiratory chain
16 supercomplex with regulatory implications.⁶⁴⁻⁶⁶
17
18
19
20
21
22
23
24
25
26
27
28
29
30
31

32 CONCLUSIONS

33
34 The current studies report a variety of new ligands that can impact a site that has
35 been defined crystallographically as a bile acid binding site in bacterial and mammalian
36 *CcO*. The results reveal the ability of certain carboxylate and non-carboxylate
37 amphipathic molecules to stimulate or inhibit E101A and WT *RsCcO*, as well as the
38 bovine enzyme, by competing for binding in this region. These ligands alter the electron
39 transfer equilibrium between heme *a* and heme *a*₃, likely by affecting proton uptake in
40 the K-path. Two overlapping sites for steroid and alkyl chain binding at the interface of
41 subunits I and II are proposed to be involved in mediating the observed effects. The
42 results suggest that this conserved site has physiological significance, although further
43
44
45
46
47
48
49
50
51
52
53
54
55
56
57
58
59
60

1
2
3 investigation by crystallography, mutagenesis, ligand screening and modeling will be
4
5 required to define the native interacting species.
6
7
8
9

10 **ACKNOWLEDGMENTS**

11
12 The authors would like to thank OpenEye Scientific Software (Santa Fe, NM³⁵)
13
14 for academic licensing of their software.
15
16
17
18
19

20 **SUPPORTING INFORMATION AVAILABLE**

21
22 Supporting Table T1 depicts the structures of the compounds tested on *RsCcO*
23
24 and discussed in this paper. Supporting Table T2 compares protein-ligand interactions in
25
26 the *bovCcO* and *RsCcO* bile acid/steroid binding sites. This material is available free of
27
28 charge via the Internet at <http://pubs.acs.org>.
29
30
31
32
33

34 **REFERENCES**

- 35
36
37 1. Tsukihara, T., Aoyama, H., Yamashita, E., Tomizaki, T., Yamaguchi, H.,
38
39 Shinzawa-Itoh, K., Nakashima, R., Yaono, R., and Yoshikawa, S. (1996) The
40
41 whole structure of the 13-subunit oxidized cytochrome *c* oxidase at 2.8 angstrom,
42
43 *Science* 272, 1136-1144.
44
45
46 2. Qin, L., Hiser, C., Mulichak, A., Garavito, R. M., and Ferguson-Miller, S. (2006)
47
48 Identification of conserved lipid/detergent-binding sites in a high-resolution
49
50 structure of the membrane protein cytochrome *c* oxidase, *Proc. Natl. Acad. Sci.*
51
52 *U.S.A.* 103, 16117-16122.
53
54
55
56
57

- 1
2
3 3. Qin, L., Sharpe, M. A., Garavito, R. M., and Ferguson-Miller, S. (2007)
4
5 Conserved lipid-binding sites in membrane proteins: a focus on cytochrome *c*
6
7
8 oxidase, *Curr. Opin. Struct. Biol.* 17, 444-450.
9
- 10 4. Koepke, J., Olkhova, E., Angerer, H., Muller, H., Peng, G., and Michel, H. (2009)
11
12 High resolution crystal structure of *Paracoccus denitrificans* cytochrome *c*
13
14 oxidase: new insights into the active site and the proton transfer pathways,
15
16
17 *Biochim. Biophys. Acta* 1787, 635-645.
18
- 19 5. Shinzawa-Itoh, K., Aoyama, H., Muramoto, K., Terada, H., Kurauchi, T.,
20
21 Tadehara, Y., Yamasaki, A., Sugimura, T., Kurono, S., Tsujimoto, K.,
22
23
24 Mizushima, T., Yamashita, E., Tsukihara, T., and Yoshikawa, S. (2007)
25
26
27 Structures and physiological roles of 13 integral lipids of bovine heart cytochrome
28
29
30 *c* oxidase, *EMBO J.* 26, 1713-1725.
31
- 32 6. Ferguson-Miller, S., Hiser, C., and Liu, J. (2012) Gating and regulation of the
33
34 cytochrome *c* oxidase proton pump, *Biochim. Biophys. Acta* 1817, 489-494.
35
- 36 7. Brierley, G. P., and Merola, A. J. (1962) Studies of Electron-Transfer System .48.
37
38 Phospholipid Requirements in Cytochrome Oxidase, *Biochim. Biophys. Acta* 64,
39
40
41 205-217.
42
- 43 8. Vanneste, W. H., Ysebaert, M., and Mason, H. S. (1974) Decline of Molecular
44
45
46 Activity of Cytochrome-Oxidase during Purification, *J. Biol. Chem.* 249, 7390-
47
48
49 7401.
50
51
52
53
54
55
56
57

- 1
2
3
4
5
6
7
8
9
10
11
12
13
14
15
16
17
18
19
20
21
22
23
24
25
26
27
28
29
30
31
32
33
34
35
36
37
38
39
40
41
42
43
44
45
46
47
48
49
50
51
52
53
54
55
56
57
58
59
60
9. Yu, C. A., Yu, L., and King, T. E. (1975) Studies on Cytochrome-Oxidase - Interactions of Cytochrome-Oxidase Protein with Phospholipids and Cytochrome-C, *J. Biol. Chem.* 250, 1383-1392.
10. Vik, S. B., and Capaldi, R. A. (1977) Lipid Requirements for Cytochrome-C Oxidase Activity, *Biochemistry* 16, 5755-5759.
11. Vik, S. B., and Capaldi, R. A. (1980) Conditions for Optimal Electron-Transfer Activity of Cytochrome-C Oxidase Isolated from Beef-Heart Mitochondria, *Biochem. Biophys. Res. Commun.* 94, 348-354.
12. Van Buuren, K. J. H., and Van Gelder, B. F. (1974) Biochemical and Biophysical Studies on Cytochrome-c Oxidase .13. Effect of Cholate on Enzymic Activity, *Biochim. Biophys. Acta* 333, 209-217.
13. Branden, M., Tomson, F., Gennis, R. B., and Brzezinski, P. (2002) The entry point of the K-proton-transfer pathway in cytochrome *c* oxidase, *Biochemistry* 41, 10794-10798.
14. Tomson, F. L., Morgan, J. E., Gu, G. P., Barquera, B., Vygodina, T. V., and Gennis, R. B. (2003) Substitutions for glutamate 101 in subunit II of cytochrome *c* oxidase from *Rhodobacter sphaeroides* result in blocking the proton-conducting K-channel, *Biochemistry* 42, 1711-1717.
15. Ma, J. X., Tsatsos, P. H., Zaslavsky, D., Barquera, B., Thomas, J. W., Katsonouri, A., Puustinen, A., Wikstrom, M., Brzezinski, P., Alben, J. O., and Gennis, R. B. (1999) Glutamate-89 in subunit II of cytochrome *bo*₃ from *Escherichia coli* is

- 1
2
3 required for the function of the heme-copper oxidase, *Biochemistry* 38, 15150-
4 15156.
5
6
7
- 8 16. Qin, L., Mills, D. A., Hiser, C., Murphree, A., Garavito, R. M., Ferguson-Miller,
9 S., and Hosler, J. (2007) Crystallographic location and mutational analysis of Zn
10 and Cd inhibitory sites and role of lipidic carboxylates in rescuing proton path
11 mutants in cytochrome *c* oxidase, *Biochemistry* 46, 6239-6248.
12
13
14
15
16
- 17 17. Konstantinov, A. A., Siletsky, S., Mitchell, D., Kaulen, A., and Gennis, R. B.
18 (1997) The roles of the two proton input channels in cytochrome *c* oxidase from
19 *Rhodobacter sphaeroides* probed by the effects of site-directed mutations on time-
20 resolved electrogenic intraprotein proton transfer, *Proc. Natl. Acad. Sci. U.S.A.*
21 94, 9085-9090.
22
23
24
25
26
27
28
- 29 18. Vygodina, T. V., Pecoraro, C., Mitchell, D., Gennis, R., and Konstantinov, A. A.
30 (1998) Mechanism of inhibition of electron transfer by amino acid replacement
31 K362M in a proton channel of *Rhodobacter sphaeroides* cytochrome *c* oxidase,
32 *Biochemistry* 37, 3053-3061.
33
34
35
36
37
38
- 39 19. Antalik, M., Jancura, D., Palmer, G., and Fabian, M. (2005) A role for the protein
40 in internal electron transfer to the catalytic center of cytochrome *c* oxidase,
41 *Biochemistry* 44, 14881-14889.
42
43
44
45
- 46 20. Frank, V., and Kadenbach, B. (1996) Regulation of the H⁺/e⁻ stoichiometry of
47 cytochrome *c* oxidase from bovine heart by intramitochondrial ATP/ADP ratios,
48 *FEBS Lett.* 382, 121-124.
49
50
51
52
53
54
55
56
57

- 1
2
3
4
5
6
7
8
9
10
11
12
13
14
15
16
17
18
19
20
21
22
23
24
25
26
27
28
29
30
31
32
33
34
35
36
37
38
39
40
41
42
43
44
45
46
47
48
49
50
51
52
53
54
55
56
57
58
59
60
21. Arnold, S., and Kadenbach, B. (1997) Cell respiration is controlled by ATP, an allosteric inhibitor of cytochrome-*c* oxidase, *Eur. J. Biochem.* *249*, 350-354.
 22. Napiwotzki, J., ShinzawaItoh, K., Yoshikawa, S., and Kadenbach, B. (1997) ATP and ADP bind to cytochrome *c* oxidase and regulate its activity, *J. Biol. Chem.* *378*, 1013-1021.
 23. Ludwig, B., Bender, E., Arnold, S., Huttemann, M., Lee, I., and Kadenbach, B. (2001) Cytochrome *c* oxidase and the regulation of oxidative phosphorylation, *ChemBioChem* *2*, 392-403.
 24. Kadenbach, B. (2003) Intrinsic and extrinsic uncoupling of oxidative phosphorylation, *Biochim. Biophys. Acta-Bioenerg.* *1604*, 77-94.
 25. Shoji, K., Giuffre, A., D'Itri, E., Hagiwara, K., Yamanaka, T., Brunori, M., and Sarti, P. (2000) The ratio between the fast and slow forms of bovine cytochrome *c* oxidase is changed by cholate or nucleotides bound to the cholate-binding site close to the cytochrome a_3/Cu_B binuclear centre, *Cell. Mol. Life Sci.* *57*, 1482-1487.
 26. Qin, L., Mills, D. A., Buhrow, L., Hiser, C., and Ferguson-Miller, S. (2008) A conserved steroid binding site in cytochrome *c* oxidase, *Biochemistry* *47*, 9931-9933.
 27. Hiser, C., Mills, D. A., Schall, M., and Ferguson-Miller, S. (2001) C-terminal truncation and histidine-tagging of cytochrome *c* oxidase subunit II reveals the native processing site, shows involvement of the C-terminus in cytochrome *c*

- 1
2
3 binding, and improves the assay for proton pumping, *Biochemistry* 40, 1606-
4
5 1615.
6
7
- 8 28. Suarez, M. D., Revzin, A., Narlock, R., Kempner, E. S., Thompson, D. A., and
9
10 Fergusonmiller, S. (1984) The Functional and Physical Form of Mammalian
11
12 Cytochrome *c* Oxidase Determined by Gel-Filtration, Radiation Inactivation, and
13
14 Sedimentation Equilibrium-Analysis, *J. Biol. Chem.* 259, 3791-3799.
15
16
- 17 29. Hosler, J. P., Fetter, J., Tecklenburg, M. M. J., Espe, M., Lerma, C., and
18
19 Fergusonmiller, S. (1992) Cytochrome *aa*₃ of *Rhodobacter sphaeroides* as a
20
21 Model for Mitochondrial Cytochrome *c* Oxidase - Purification, Kinetics, Proton
22
23 Pumping, and Spectral-Analysis, *J. Biol. Chem.* 267, 24264-24272.
24
25
- 26 30. Dailey, H. A., Wu, C. K., Horanyi, P., Medlock, A. E., Najahi-Missaoui, W.,
27
28 Burden, A. E., Dailey, T. A., and Rose, J. (2007) Altered orientation of active site
29
30 residues in variants of human ferrochelatase. Evidence for a hydrogen bond
31
32 network involved in catalysis, *Biochemistry* 46, 7973-7979.
33
34
- 35 31. Medlock, A. E., Dailey, T. A., Ross, T. A., Dailey, H. A., and Lanzilotta, W. N.
36
37 (2007) A pi-helix switch selective for porphyrin deprotonation and product
38
39 release in human ferrochelatase, *J. Mol. Biol.* 373, 1006-1016.
40
41
- 42 32. Zunszain, P. A., Ghuman, J., McDonagh, A. F., and Curry, S. (2008)
43
44 Crystallographic analysis of human serum albumin complexed with 4Z,15E-
45
46 bilirubin-IX alpha, *J. Mol. Biol.* 381, 394-406.
47
48
49
50
51
52
53
54
55
56
57

- 1
2
3
4
5
6
7
8
9
10
11
12
13
14
15
16
17
18
19
20
21
22
23
24
25
26
27
28
29
30
31
32
33
34
35
36
37
38
39
40
41
42
43
44
45
46
47
48
49
50
51
52
53
54
55
56
57
58
59
60
33. Schnecke, V., Swanson, C. A., Getzoff, E. D., Tainer, J. A., and Kuhn, L. A. (1998) Screening a peptidyl database for potential ligands to proteins with side-chain flexibility, *Proteins: Struct. Funct. Genet.* *33*, 74-87.
34. Zavodszky, M. I., Sanschagrin, P. C., Korde, R. S., and Kuhn, L. A. (2002) Distilling the essential features of a protein surface for improving protein-ligand docking, scoring, and virtual screening, *J. Comp. Aid. Mol. Des.* *16*, 883-902.
35. Hawkins, P. C. D., Skillman, A. G., Warren, G. L., Ellingson, B. A., and Stahl, M. T. (2010) Conformer Generation with OMEGA: Algorithm and Validation Using High Quality Structures from the Protein Databank and Cambridge Structural Database, *J. Chem. Inf. Model.* *50*, 572-584.
36. Landau, M., Mayrose, I., Rosenberg, Y., Glaser, F., Martz, E., Pupko, T., and Ben-Tal, N. (2005) ConSurf 2005: the projection of evolutionary conservation scores of residues on protein structures, *Nucleic Acids Res.* *33*, W299-W302.
37. Jacobs, D. J., Rader, A. J., Kuhn, L. A., and Thorpe, M. F. (2001) Protein flexibility predictions using graph theory, *Proteins: Struct. Funct. Genet.* *44*, 150-165.
38. Buhrow, L., Ferguson-Miller, S., and Kuhn, L. A. (2012) From Static Structure to Living Protein: Computational Analysis of Cytochrome *c* Oxidase Main-chain Flexibility, *Biophys. J.* *102*, 2158-2166.
39. Fetter, J., Sharpe, M., Qian, J., Mills, D., Ferguson-Miller, S., and Nicholls, P. (1996) Fatty acids stimulate activity and restore respiratory control in a proton channel mutant of cytochrome *c* oxidase, *FEBS Lett.* *393*, 155-160.

- 1
2
3
4
5
6
7
8
9
10
11
12
13
14
15
16
17
18
19
20
21
22
23
24
25
26
27
28
29
30
31
32
33
34
35
36
37
38
39
40
41
42
43
44
45
46
47
48
49
50
51
52
53
54
55
56
57
58
59
60
40. Verhoeven, N. M., Wanders, R. J., Poll-The, B. T., Saudubray, J. M., and Jakobs, C. (1998) The metabolism of phytanic acid and pristanic acid in man: a review, *J. Inherited Metab. Dis.* *21*, 697-728.
41. Kruska, N., and Reiser, G. (2011) Phytanic acid and pristanic acid, branched-chain fatty acids associated with Refsum disease and other inherited peroxisomal disorders, mediate intracellular Ca^{2+} signaling through activation of free fatty acid receptor GPR40, *Neurobiol. Dis.* *43*, 465-472.
42. Hellgren, L. I. (2010) Phytanic acid--an overlooked bioactive fatty acid in dairy fat?, *Ann. N.Y. Acad. Sci.* *1190*, 42-49.
43. Amengual, J., Ribot, J., Bonet, M. L., and Palou, A. (2008) Retinoic acid treatment increases lipid oxidation capacity in skeletal muscle of mice, *Obesity* *16*, 585-591.
44. Rosevear, P., VanAken, T., Baxter, J., and Ferguson-Miller, S. (1980) Alkyl glycoside detergents: a simpler synthesis and their effects on kinetic and physical properties of cytochrome *c* oxidase, *Biochemistry* *19*, 4108-4115.
45. Mahapatro, S. N., and Robinson, N. C. (1990) Effect of Changing the Detergent Bound to Bovine Cytochrome-*c* Oxidase Upon Its Individual Electron-Transfer Steps, *Biochemistry* *29*, 764-770.
46. Howell, S. C., Mittal, R., Huang, L. J., Travis, B., Breyer, R. M., and Sanders, C. R. (2010) CHOBIMALT: A Cholesterol-Based Detergent, *Biochemistry* *49*, 9572-9583.

- 1
2
3
4
5
6
7
8
9
10
11
12
13
14
15
16
17
18
19
20
21
22
23
24
25
26
27
28
29
30
31
32
33
34
35
36
37
38
39
40
41
42
43
44
45
46
47
48
49
50
51
52
53
54
55
56
57
58
59
60
47. Vanneste, W. H. (1966) Stoichiometry and Absorption Spectra of Components a and a_3 in Cytochrome c Oxidase, *Biochemistry* 5, 838-848.
48. Qin, L., Liu, J., Mills, D. A., Proshlyakov, D. A., Hiser, C., and Ferguson-Miller, S. (2009) Redox-Dependent Conformational Changes in Cytochrome c Oxidase Suggest a Gating Mechanism for Proton Uptake, *Biochemistry* 48, 5121-5130.
49. Liu, J. A., Qin, L., and Ferguson-Miller, S. (2011) Crystallographic and online spectral evidence for role of conformational change and conserved water in cytochrome oxidase proton pump, *Proc. Natl. Acad. Sci. U.S.A.* 108, 1284-1289.
50. Sharpe, M. A., Qin, L., and Ferguson-Miller, S. (2005) Proton Entry, Exit and Pathways in Cytochrome Oxidase: Insight from Conserved Water, In *Biophysical and Structural Aspects of Bioenergetics* (Wikstrom, M., Ed.), pp 26-54, The Royal Society of Chemistry, Cambridge, UK, Cambridge.
51. Sharpe, M. A., and Ferguson-Miller, S. (2008) A chemically explicit model for the mechanism of proton pumping in heme-copper oxidases, *J. Bioenerg. Biomembr.* 40, 541-549.
52. Busenlehner, L. S., Salomonsson, L., Brzezinski, P., and Armstrong, R. N. (2006) Mapping protein dynamics in catalytic intermediates of the redox-driven proton pump cytochrome c oxidase, *Proc. Natl. Acad. Sci. U.S.A.* 103, 15398-15403.
53. Fendel, U., Tocilescu, M. A., Kerscher, S., and Brandt, U. (2008) Exploring the inhibitor binding pocket of respiratory complex I, *Biochim. Biophys. Acta-Bioenerg.* 1777, 660-665.

- 1
2
3 54. Okun, J. G., Lummen, P., and Brandt, U. (1999) Three classes of inhibitors share
4 a common binding domain in mitochondrial complex I (NADH:ubiquinone
5 oxidoreductase), *J. Biol. Chem.* 274, 2625-2630.
6
7
8
9
10 55. Simon, N., Jolliet, P., Morin, C., Zini, R., Urien, S., and Tillement, J. P. (1998)
11 Glucocorticoids decrease cytochrome *c* oxidase activity of isolated rat kidney
12 mitochondria, *FEBS Lett.* 435, 25-28.
13
14
15 56. Molano, F., Saborido, A., Delgado, J., Moran, M., and Megias, A. (1999) Rat
16 liver lysosomal and mitochondrial activities are modified by anabolic-androgenic
17 steroids, *Med. Sci. Sports Exer.* 31, 243-250.
18
19
20
21
22 57. Starkov, A. A., Simonyan, R. A., Dedukhova, V. I., Mansurova, S. E.,
23 Palamarchuk, L. A., and Skulachev, V. P. (1997) Regulation of the energy
24 coupling in mitochondria by some steroid and thyroid hormones, *Biochim.*
25 *Biophys. Acta-Bioenerg.* 1318, 173-183.
26
27
28
29
30
31
32
33 58. Vaz, A. R., Delgado-Esteban, M., Brito, M. A., Bolanos, J. P., Brites, D., and
34 Almeida, A. (2010) Bilirubin selectively inhibits cytochrome *c* oxidase activity
35 and induces apoptosis in immature cortical neurons: assessment of the protective
36 effects of glyoursodeoxycholic acid, *J. Neurochem.* 112, 56-65.
37
38
39
40
41
42
43 59. Malik, S. G., Irwanto, K. A., Ostrow, J. D., and Tiribelli, C. (2010) Effect of
44 bilirubin on cytochrome *c* oxidase activity of mitochondria from mouse brain and
45 liver, *BMC Res. Notes* 3, 162-167.
46
47
48
49
50 60. Goglia, F. (2005) Biological effects of 3,5-diiodothyronine (T-2), *Biochemistry-*
51 *Moscow* 70, 164-172.
52
53
54
55
56
57
58
59
60

- 1
2
3
4
5
6
7
8
9
10
11
12
13
14
15
16
17
18
19
20
21
22
23
24
25
26
27
28
29
30
31
32
33
34
35
36
37
38
39
40
41
42
43
44
45
46
47
48
49
50
51
52
53
54
55
56
57
58
59
60
61. Arnold, S., Goglia, F., and Kadenbach, B. (1998) 3,5-Diiodothyronine binds to subunit Va of cytochrome-*c* oxidase and abolishes the allosteric inhibition of respiration by ATP, *Eur. J. Biochem.* 252, 325-330.
62. Busanello, E. N. B., Viegas, C. M., Moura, A. P., Tonin, A. M., Grings, M., Vargas, C. R., and Wajner, M. (2010) In vitro evidence that phytanic acid compromises Na⁺, K⁺-ATPase activity and the electron flow through the respiratory chain in brain cortex from young rats, *Brain Res.* 1352, 231-238.
63. Kadenbach, B., Napiwotzki, J., Frank, V., Arnold, S., Exner, S., and Huttemann, M. (1998) Regulation of energy transduction and electron transfer in cytochrome *c* oxidase by adenine nucleotides, *J. Bioenerg. Biomembr.* 30, 25-33.
64. Dudkina, N. V., Kouril, R., Peters, K., Braun, H. P., and Boekema, E. J. (2010) Structure and function of mitochondrial supercomplexes, *Biochim. Biophys. Acta* 1797, 664-670.
65. Althoff, T., Mills, D. J., Popot, J. L., and Kuhlbrandt, W. (2011) Arrangement of electron transport chain components in bovine mitochondrial supercomplex I₁III₂IV₁, *EMBO J.* 30, 4652-4664.
66. Bottinger, L., Horvath, S. E., Kleinschroth, T., Hunte, C., Daum, G., Pfanner, N., and Becker, T. (2012) Phosphatidylethanolamine and Cardiolipin Differentially Affect the Stability of Mitochondrial Respiratory Chain Supercomplexes, *J. Mol. Biol.* 423, 677-686.

TABLES

Table 1. Effects of bile acids on the activity of the E101A mutant and WT *RsCcO*

Bile Acid Additive	<i>RsCcO</i> E101A Activity ($e^-/\text{sec}/aa_3$)	<i>RsCcO</i> WT Activity ($e^-/\text{sec}/aa_3$)
Buffer	60 ± 10	1270 ± 20
Cholate	800 ± 10	1260 ± 10
Deoxycholate (DOC)	780 ± 20	1210 ± 20
ChenoDOC	620 ± 60	1240 ± 30
Lithocholate*	530 ± 60	1150 ± 80
Taurocholate	150 ± 10	1360 ± 80
GlycoursoDOC (GUDCA)	90 ± 40	1160 ± 40
GlycochenoDOC	60 ± 30	1360 ± 60
UrsoDOC	50 ± 10	1260 ± 60

Purified *RsCcO* was assayed in 0.06% DDM as described in Materials and Methods in the absence (Buffer) or presence of 250 μM of each bile acid. All numbers are means \pm one standard deviation of at least 3 assays. * Due to its poor solubility, lithocholate was added to a final concentration of only 75 μM .

FIGURE LEGENDS

Figure 1. Stimulation of E101A *RsCcO* by amphipathic carboxylates in 0.06% DDM.

Purified E101A *RsCcO* was assayed in 0.06% DDM as described in Materials and Methods. Panel A: bilirubin (BR; red), cholate (purple), cholesteryl hemisuccinate (CHS; green), deoxycholate (DOC; black), protoporphyrin IX (PPIX; magenta). Panel B: arachidonic acid (cyan), docosahexanoic acid (blue), phytanic acid (orange), retinoic acid (brown). Note different concentration and activity axes in panels A and B; higher affinity ligands are shown in panel B. The starting activities in the absence of ligand ranged from 31-66 s⁻¹.

Figure 2. Effects of DDM (A) and amphipathic carboxylates in low DDM (B). Purified E101A (circles) and WT (triangles) *RsCcO* were assayed in 0.01% DDM as described in Materials and Methods. Additive in panel A: DDM; additives in panel B: cholesteryl hemisuccinate (CHS; open circles, dashed line), deoxycholate (DOC; solid circles, solid line), retinoic acid (half-filled circles, dotted line).

Figure 3. Inhibition of *RsCcO* by lysolipids and detergents. Purified E101A (A,C) and WT (B) *RsCcO* were assayed in 0.01% DDM (A,B) and 0.06% DDM (C) as described in Materials and Methods. Additives: CHOBIMALT (red), C12E8 (purple), lyso-PC (black), Triton X100 (blue), Tween 20 (green).

1
2
3 **Figure 4.** Competition of Triton X100 (A) and CHOBIMALT (B) with deoxycholate
4 (DOC) for activation of E101A *R_sCcO*. Purified E101A *R_sCcO* was assayed in 0.01%
5 (DOC) for activation of E101A *R_sCcO*. Purified E101A *R_sCcO* was assayed in 0.01%
6 DDM as described in Materials and Methods in the absence (solid circles) and presence
7 (open circles) of 300 μ M DOC.
8
9

10
11
12
13
14 **Figure 5.** Spectra of purified E101A and WT *CcO* with and without CHOBIMALT.
15 Panel A: Soret region; panel B: α region. Spectra were normalized to the fully reduced α
16 peak height at 607nm - 630nm. Spectra of fully oxidized and fully reduced purified *CcO*
17 are shown in black. Steady-state spectra in 100mM CHES pH 9.5 with 0.01% DDM
18 were recorded 3 minutes after adding 1 mM ascorbate and 200 μ M TMPD: WT only
19 (green), WT with CHOBIMALT (blue), E101A only (magenta), E101A with
20 CHOBIMALT (red).
21
22
23
24
25
26
27
28
29
30
31
32
33

34 **Figure 6.** Potential binding orientations of known amphipathic ligands in the *R_sCcO*
35 steroid binding site. (A) Heme (magenta sticks) and cholate (black sticks) bound in the
36 same site in two different crystal structures of ferrochelatase (PDB: 2PO7³⁰ and 2QD2
37 ³¹). (B) An energetically favorable orientation of the BR analog biliverdin (red sticks) in
38 *R_sCcO* based on ligand transposition from serum albumin. Energetically favorable
39 *SLIDE* dockings into *R_sCcO* of (C) PPIX (magenta sticks), (D) BR (red sticks), and (E)
40 two DDM flexible conformers (yellow and magenta sticks). (B-E) The
41 crystallographically bound deoxycholate (black sticks; PDB: 3DTU²⁶) and DDM (blue
42 sticks; PDB 3HB3⁴) are shown as reference molecules.
43
44
45
46
47
48
49
50
51
52
53
54
55
56
57
58
59
60

1
2
3
4
5
6 **Figure 7.** *RsCcO* deoxycholate binding site with conserved residues and bound water
7 molecules (PDB 3DTU²⁶). The steroid binding site side chains are colored by degree of
8 conservation in *CcO* sequences as calculated in Buhrow *et al.*³⁸ where residues with
9 >75%, 50-75%, or less than 50% conservation are colored dark blue, medium blue, and
10 gray, respectively. The structure includes a bound deoxycholate (green sticks), K-path
11 water molecules (red spheres), and a cadmium ion (orange sphere).
12
13
14
15
16
17
18
19
20
21

22 **Figure 8.** *RsCcO* K-path rigidification upon ligand binding. (A) *RsCcO* (PDB: 2GSM²)
23 and (B) deoxycholate-bound *RsCcO* (PDB: 3DTU²⁶) are colored by crystallographic B-
24 value, where red represents values $\geq 65 \text{ \AA}^2$, while deep blue represents values $\leq 35 \text{ \AA}^2$.
25
26 (C) *RsCcO* and (D) deoxycholate-bound *RsCcO* are colored by internal protein flexibility
27 as determined by the *ProFlex*. Deep blue represents greatest rigidity while red represents
28 greatest flexibility.
29
30
31
32
33
34
35
36
37
38

39 **Figure 9.** Two-site model for binding of steroids and detergents near the K-path
40 entrance. The lower site is shown with the crystallographic deoxycholate in yellow (from
41 *RsCcO*, PDB: 3DTU²⁶). The upper site is shown with the crystallographic DDM in green
42 (from *PdCcO*, PDB: 3HB3⁴) modeled with the flexible head group in the most extended
43 position. The surface of the *RsCcO* structure is represented with the hydrophobic regions
44 in dark orange, the hydrophilic charged regions in blue, and neutral regions in pale
45
46
47
48
49
50
51
52
53
54
55
56
57
58
59
60

1
2
3 blue/pale orange/white (Chimera, UCSF). The position of the membrane region is
4
5 indicated by blue lines.
6
7
8
9
10
11
12
13
14
15
16
17
18
19
20
21
22
23
24
25
26
27
28
29
30
31
32
33
34
35
36
37
38
39
40
41
42
43
44
45
46
47
48
49
50
51
52
53
54
55
56
57
58
59
60

FIGURES

Figure 1.

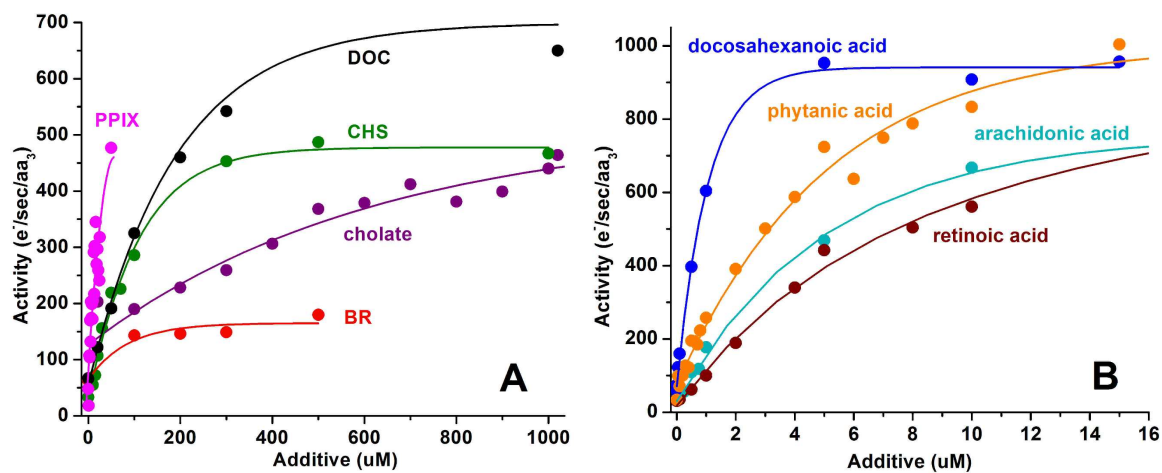


Figure 2.

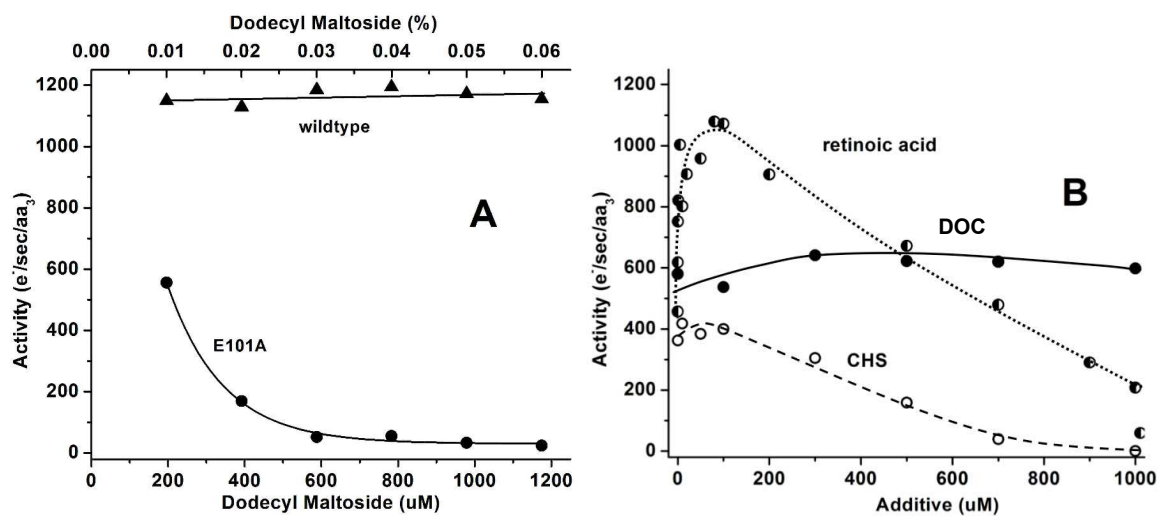


Figure 3.

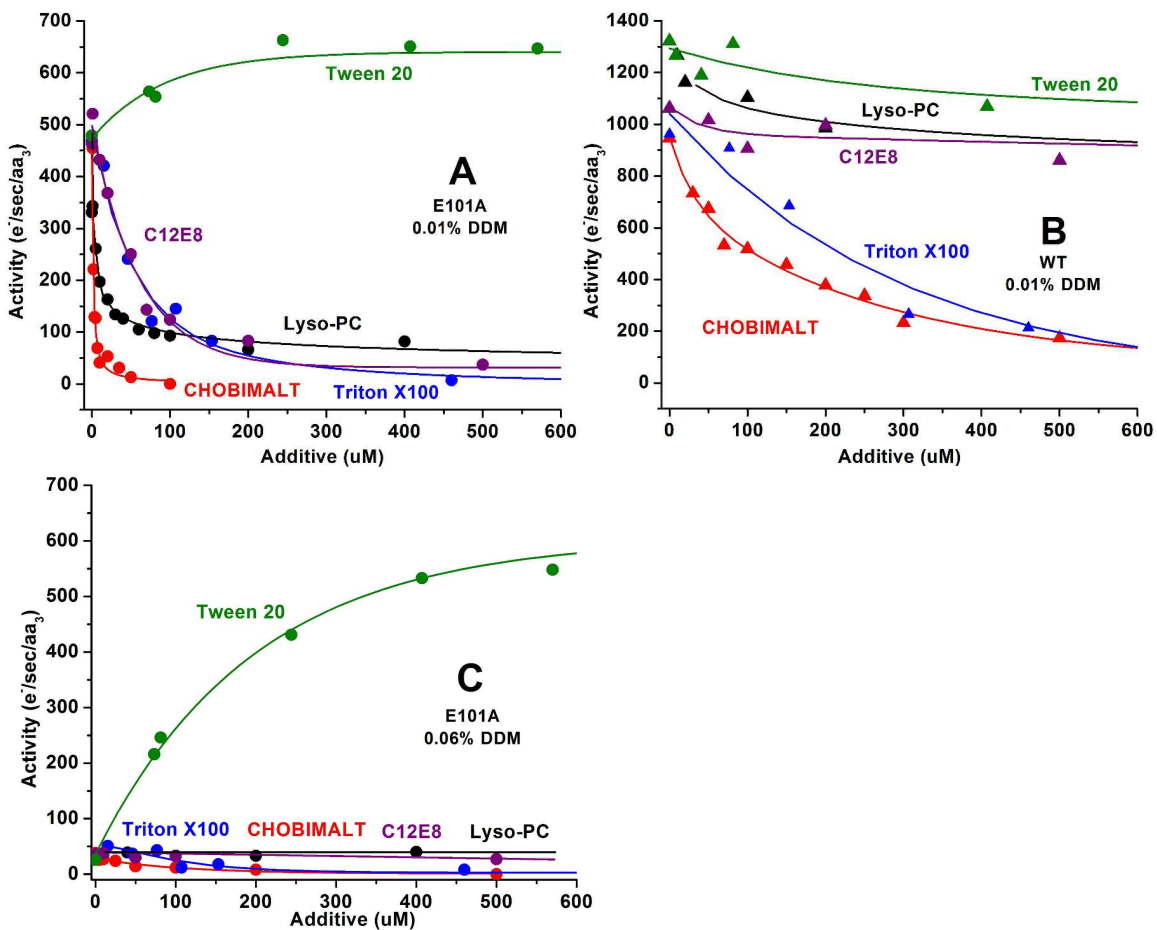
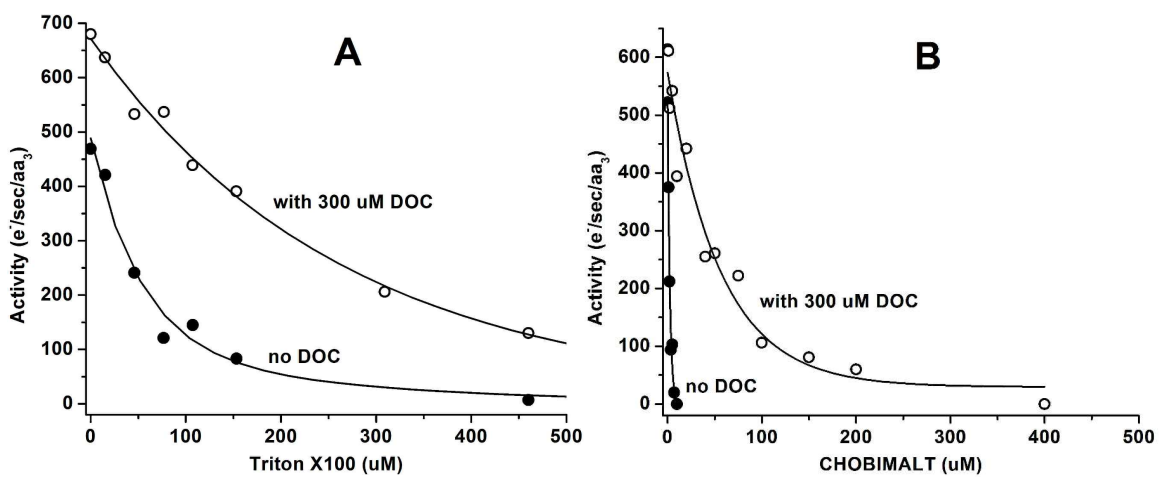


Figure 4.



43

Figure 5.

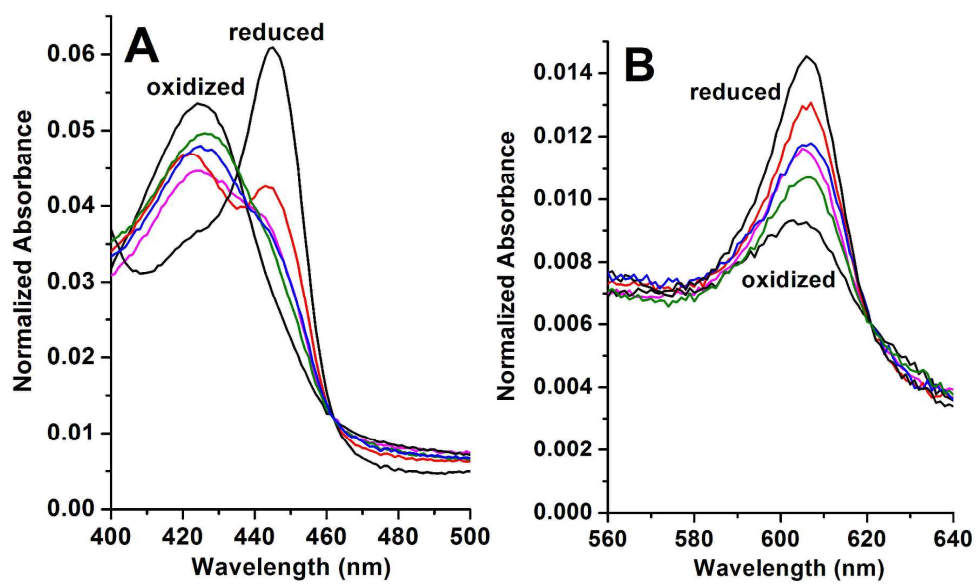


Figure 8.

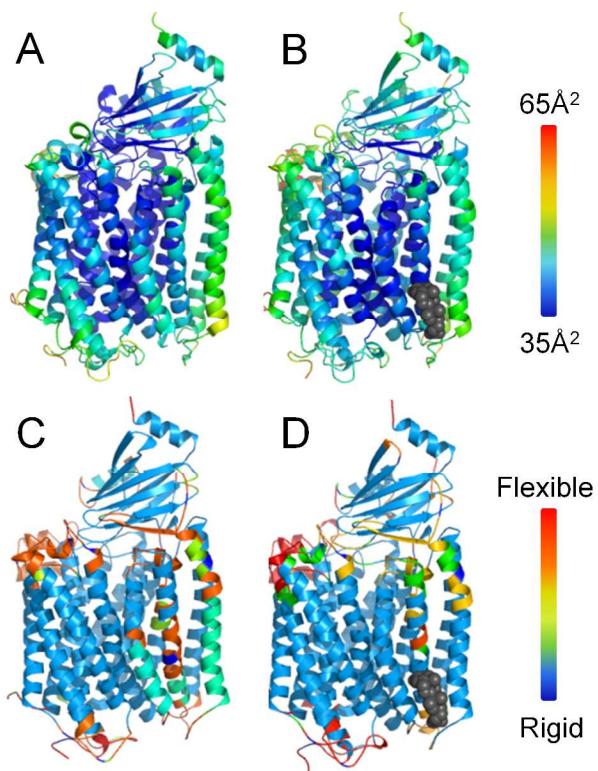
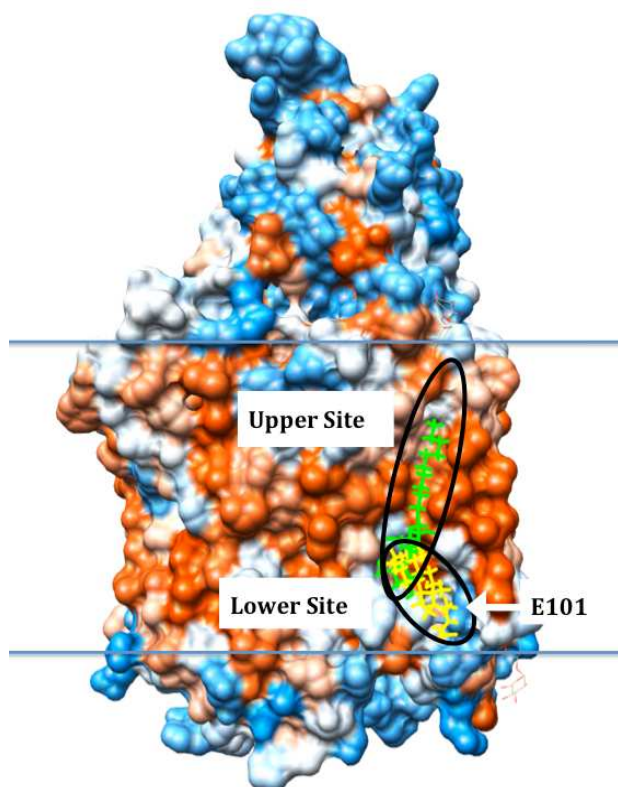


Figure 9.



1
2
3 **FOR TABLE OF CONTENTS USE ONLY**
4
5
6

7 Graphic for table of contents for the following manuscript:
8
9

10 **A Conserved Amphipathic Ligand Binding Region Influences K-Path Dependent**
11 **Activity of Cytochrome *c* Oxidase.**
12
13

14
15 Carrie Hiser, Leann Buhrow, Jian Liu, Leslie Kuhn and Shelagh Ferguson-Miller
16

17 Department of Biochemistry and Molecular Biology, Michigan State University, East
18

19 Lansing, Michigan 48824, USA
20
21
22
23
24
25
26
27
28
29
30
31
32
33
34

